Available online at www.sciencedirect.com
ScienceDirect
Trans. Nonferrous Met. Soc. China 34(2024) 1976−1993
Transactions of Nonferrous Metals Society of China
www.tnmsc.cn

Efficient mechanochemical leaching of zinc from zinc oxide ores

Yu-sen YU[1,2], Li-xue CUI[1,2], Li-bo ZHANG[1,2], Yun-fan WANG[1,2]

1. Faculty of Metallurgical and Energy Engineering, Kunming University of Science and Technology, Kunming 650093, China;
2. State Key Laboratory of Complex Nonferrous Metal Resources Clean Utilization, Kunming University of Science and Technology, Kunming 650093, China

Received 6 January 2023; accepted 18 September 2023

Abstract: A basket grinder was used as mechanochemical activation equipment to study low-grade lead–zinc oxide ores in the Lanping area, China and a mechanochemical leaching (MCL) process combining grinding with NaOH solution leaching was proposed for zinc leaching. The effects of leaching temperature, NaOH concentration, leaching time, liquid–solid ratio, and stirring speed on zinc leaching rate were investigated. Experimental results show that under the optimal conditions, the zinc leaching rate of MCL reaches 92.3%, which is 7.2% higher than that of conventional stirring leaching (CSL). And small difference in energy consumption is observed between the two processes, indicating the superiority of MCL. The strengthening mechanism of mechanochemical activation was investigated by analyzing the zinc phase of raw ore, and XRD, SEM−EDS, EPMA and particle size analyses were conducted on leaching residues from different processes under the optimal conditions.

Key words: mechanochemical leaching; mechanical activation; alkaline leaching; zinc oxide ore; basket grinder

1 Introduction

Zinc is an important strategic base metal and is the third most consumed nonferrous metal following aluminum and copper [1,2]. At present, the zinc smelting industry is dominated by zinc sulfide [3]. With the continuous consumption of high-grade zinc sulfide ore, the growing demand for zinc has become difficult to meet, and the development and utilization of zinc oxide ore resources has become increasingly important [4]. Although China has abundant zinc oxide ore resources, especially Lanping Lead−Zinc Mine in Yunnan Province, the distribution characteristics of zinc oxide ore resources and their own characteristics (such as difficult to concentrate, high silicon, and high iron) lead to difficulty in relevant processing and smelting technologies [2,5]. Thus, methods for the economic and effective development and utilization of zinc oxide ores are of great significance.

The hydrometallurgical technology of zinc oxide ores can be divided into acid, ammonia, and alkali leaching [6−8]. Sulfuric acid leaching is the most feasible and widely applied in the industry; however, it is unsuitable for low-grade zinc oxide ores mainly because these ores contain large amount of impurity metals (such as iron and aluminum), alkaline gangue (such as CaO and MgO), and silicate components that increase the consumption of sulfuric acid and generate silica gel, which affects separation and complicates purification [2,9]. Although ammonia leaching has low zinc leaching rate when zinc silicate ore is leached [1], this process can avoid the shortcomings

Corresponding author: Yun-fan WANG, Tel: +86-18587191805, E-mail: kmustwyf@163.com
DOI: 10.1016/S1003-6326(24)66520-9

of sulfuric acid leaching. For example, zinc leaching has no silica gel problem and can achieve selective zinc leaching. However, this method is associated with large ammonia loss and poor operating environment due to the volatility of ammonia. The relevant process is still immature and remains in the laboratory research and development stage. Alkali leaching mainly refers to NaOH leaching. Although its process flow is similar to that of sulfuric acid leaching, it can avoid the shortcomings of acid leaching. Alkali leaching has the advantages of slow equipment corrosion, simple solid–liquid separation, and easy leaching solution purification. In contrast to ammonia leaching, alkali leaching will not cause environmental pollution; however, the low leaching rate of zinc silicate restricts further application of alkaline leaching for zinc oxide ores [7,10]. Therefore, an enhanced leaching method is urgently needed to improve the alkaline leaching efficiency of zinc oxide ores.

With the development of mechanochemistry, researchers have gradually realized that adding mechanical energy to minerals can change their physical and chemical properties and thereby enhance their reactivity [11,12]. As a pretreatment method, mechanical activation is widely used in the intensive leaching of minerals to improve the leaching rate of valuable metals [13−16]. XIANG et al [17] significantly improved the vanadium leaching efficiency and made the production process cleaner by combining mechanical activation pretreatment, calcification roasting, and two-step acid leaching of vanadium bearing converter slag. The mechanical activation of chalcopyrite can improve the copper extraction rate. Thus, scholars have studied the leaching behavior and mechanism of chalcopyrite [18−21]. FAN et al [22] used a planetary mill to mechanically activate indium-bearing zinc ferrite and employed SO_2 as a reducing and leaching agent. The results showed that mechanical activation can reduce the activation energy of zinc and indium. However, these studies used mechanical activation for mineral pretreatment and did not combine it with leaching. ZHANG and ZHAO [23] found that the zinc leaching effect of mechanochemical leaching (simultaneous grinding and leaching) is better than that of mechanical activation and subsequent leaching of sphalerite with alkaline solution containing $PbCO_3$. ZHAO et al [24] extracted zinc from hemimorphite by mechanochemical leaching in NaOH solution and achieved zinc leaching rate as high as 93.6% under the optimal conditions.

In this work, low-grade lead–zinc oxide ores from Lanping, Yunnan Province, China, were used as raw materials, and NaOH solution was used as a leaching agent. A basket grinder was employed as mechanochemical activation equipment to improve the alkaline leaching efficiency of zinc oxide ores through grinding while leaching. The process conditions were optimized. Compared with conventional stirring leaching (CSL), mechano-chemical leaching (MCL) can shorten leaching time, reduce reaction conditions, and improve zinc leaching rate. The strengthening mechanism of MCL was explored through leaching experiment, XRD, SEM–EDS, particle size analysis, and EPMA characterization analysis of leaching residues.

2 Experimental

2.1 Materials

The samples used in this experiment were raw, brown-yellow, low-grade lead–zinc oxide ores collected from Lanping area, Yunnan Province, China. The raw ore samples were crushed by a jaw crusher, dried in an oven, finely ground by a crusher, and sieved until the particle size was less than 150 μm. The main chemical composition of the lead–zinc oxide ore powder was detected using chemical analysis methods, and the result is presented in Table 1. Zinc phase distribution was determined using selective dissolution method as shown in Table 2. Analytical reagent (NaOH) was purchased from Tianjin Zhiyuan Chemical Reagent Co., Ltd., China.

The related characterization results of the raw ores are shown in Fig. 1. The main metal minerals in the lead–zinc oxide ores are smithsonite, cerussite, galena, and magnetite, and the gangue components are calcite and quartz (Fig. 1(a)). The particle size distribution diagram of the raw ores is shown in Fig. 1(b), and the specific granularity data are displayed in Table 3. The average particle size

Table 1 Chemical composition of lead–zinc oxide ores (wt.%)

Zn	Fe	Pb	S	SiO_2	Al_2O_3	MgO	CaO	Others
10.47	10.54	9.09	1.07	10.22	0.94	0.34	13.25	44.08

Table 2 Phase distribution of zinc in lead–zinc oxide ores

Phase composition	Zinc content/wt.%	Phase composition proportion/%
$ZnCO_3$	8.96	85.58
Zn_2SiO_4	0.47	4.49
ZnS	0.79	7.54
$ZnFe_2O_4$	0.25	2.39
Zn_T	10.47	100

of the raw ores is 56.624 μm, and the specific surface area is 0.852 m^2/g. The micromorphology is different; the sample appear as a block with irregular form or in long strips and diamond, and the particle surface is relatively smooth (Figs. 1(c) and (d)). The SEM–EDS analysis results of raw ores are shown in Fig. 2. Various elements are irregularly distributed in the raw ore. Some long crystals are composed of $CaCO_3$ and Fe_3O_4 (Point *A*), and zinc exists in the form of $ZnCO_3$ (Point *B*). On the basis of the EDS analysis of Point *C*, plumbum exists in the forms of $PbCO_3$ and PbS and silicon exists in the form of SiO_2 (Fig. 2(a)). The EDS mapping analysis of the raw ores is shown in Fig. 2(b). The distribution of C, O, Si, S, Ca, Fe, Zn, and Pb in the raw ore is uneven, revealing the complex composition of the sample.

2.2 Experimental procedure

MCL and CSL experiments were carried out under atmospheric pressure using a basket grinder as the mechanical activation device. The working principle of the device is to stir, disperse, and remix the solution and mineral powder in the barrel with the help of the agitator. The mixed materials were

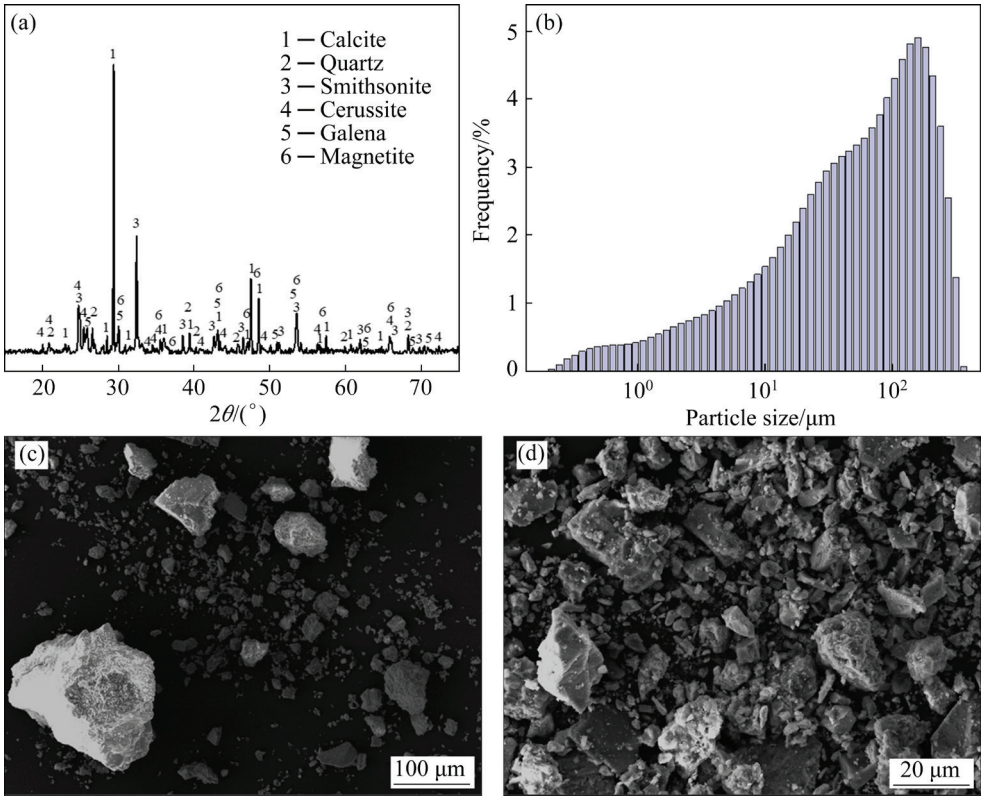

Fig. 1 Related characterization results of raw ores: (a) XRD pattern; (b) particle size distribution diagram; (c, d) SEM images

Table 3 Particle size distribution and specific surface area of raw ores

D_{10}/μm	D_{50}/μm	D_{90}/μm	$D_{3,2}$/μm	$D_{4,3}$/μm	$S_G/(m^2 \cdot g^{-1})$
3.711	56.624	193.057	7.042	78.149	0.852

D_{10}, D_{50} and D_{90} are the particle sizes corresponding to the cumulative particle size distribution of the sample reaching 10%, 50%, and 90%, respectively; $D_{3,2}$ and $D_{4,3}$ are the surface area moment mean diameter and the volume moment mean diameter, respectively; S_G is specific surface area

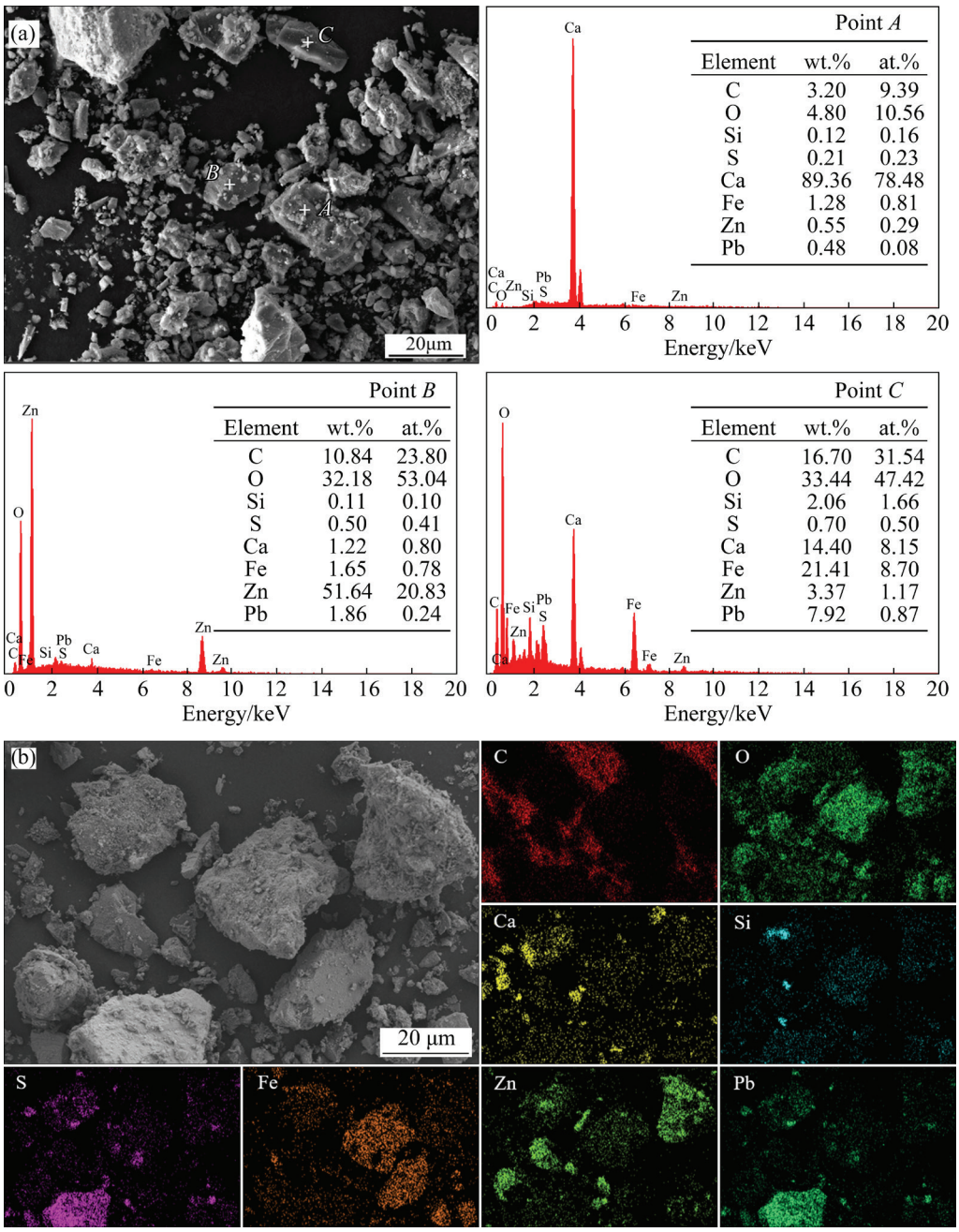

Fig. 2 SEM−EDS analysis results of raw ores: (a) Point scanning; (b) Mappings

sucked into the grinding basket through the suction pump wheel. Under the high-speed operation of the motor-driven rotating shaft and transmission shaft, the internal paddle moved the zirconia balls to rotate at high speed in the grinding basket chamber to achieve high-energy ball milling and refining. The refined materials were then discharged from the bottom of the grinding basket through the micropores in the separator and reentered the barrel. This process was repeated to achieve grinding while leaching. The schematic diagram of the device is shown in Fig. 3. In MCL, a fixed amount of zirconia balls were added to the grinding basket to serve as the grinding medium. By contrast, in CSL, no grinding medium was added. A series of comparative experiments were carried out under the same conditions to compare the performance of MCL and CSL. In brief, 150 g of *d*2 mm zirconia ball was placed into the grinding basket and 900 mL NaOH solution was added into the barrel. Different factors affecting zinc leaching were optimized: leaching temperature (45−85 °C), concentration of NaOH solution (1−5 mol/L), leaching time (10−90 min), liquid−solid ratio (5:1−15:1 mL/g), and stirring speed

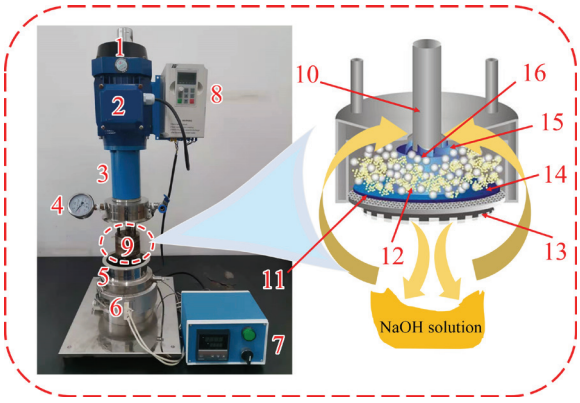

Fig. 3 Schematic diagram of basket grinder (1−Radiator; 2−Electromotor; 3−Rotating shaft; 4−Vacuum pressure gauge; 5−Charging barrel; 6−Electric heating sleeve; 7−Temperature control device; 8−Grinding control device; 9−Grinding basket; 10−Drive shaft; 11−Separator; 12−Raw ore powder; 13−Agitator; 14−Grinding basket chamber; 15−Suction pump wheel; 16−Zirconia ball)

(200−1000 r/min). After the leaching was completed, the sample was filtered while hot. The filter residue was washed with distilled water three times to obtain clean leached residue. An appropriate amount of leached solution was obtained for the detection of zinc concentration. Finally, the leached residue was dried at 100 °C for 24 h and subjected to XRD, SEM, particle size analysis, and EPMA characterization.

2.3 Characterization and analysis

The concentration of zinc in the solid samples and solutions was measured against the national standard. High zinc content was determined by EDTA volumetric method, and low zinc content was determined by atomic absorption spectrometry (AAS). The surface microstructure of the solid phase was evaluated using a scanning electron microscopy (SEM, Tescan Mira Lms, Czech Republic) and energy dispersive spectroscopy (EDS, Oxford). The particle size distribution of the solid samples was determined by particle size analyzer (Malvern 2000). The main element distribution of leaching residue was determined by EPMA (JXA−8530F Plus). The working energy consumption in the leaching process was measured with a power meter (PY-G8). Zinc leaching rate was calculated by Eq. (1). The zinc extraction efficiency was calculated by Eq. (2) [19]. According to different processes, this index can be divided into the grinding efficiency of MCL and the leaching efficiency of CSL:

$$L=\frac{CV}{m\omega_{Zn}}\times 100\% \tag{1}$$

$$\eta=\frac{C}{Pt} \tag{2}$$

where L is the zinc leaching rate, C is the Zn concentration in leaching solution (g/L), V is the volume of the corresponding filtrate after leaching (L), m is the mass of sample (g), ω_{Zn} is the zinc content in sample (%), η is the zinc extraction efficiency and can be divided into MCL grinding efficiency or CSL leaching efficiency (g/(L·h·kW), P is the rated working power of the basket grinder (kW), and t is the grinding time or leaching time (h).

The mineral compositions of lead–zinc oxide ores and leaching residue were characterized by X-ray diffractometer (XRD, Cu K_α; wavelength of λ=1.5406 Å; step size of 0.02°; time per step: 3 s; scanning range: 10°−90°; scan speed: 8 (°)/min; Panalytical, Netherlands). After the XRD patterns were deconvoluted by Jade6, the peak intensity and full width at half maximum (FWHM) were obtained through data analysis [25,26]. The amorphization degree (A) of mechanochemical leaching residue (MCLR) was calculated by Eq. (3) [11,26−28]:

$$A=100-X=100-\left(\frac{U_0 I_X}{U_X I_0}\right)\times 100 \tag{3}$$

where X is the degree of crystallinity, U_0 and U_X are the background intensities of non-activated (raw ore) and activated (MCLR) samples, respectively, and I_0 and I_X are the integral intensities of non-activated (raw ore) and activated (MCLR) samples, respectively.

3 Results and discussion

The effects of leaching temperature, NaOH concentration, leaching time, liquid–solid ratio, and stirring speed on zinc leaching rate in MCL and CSL were studied, as shown in Fig. 4. The effects of different leaching conditions on zinc extraction efficiency in MCL and CSL were also determined, as shown in Fig. 5.

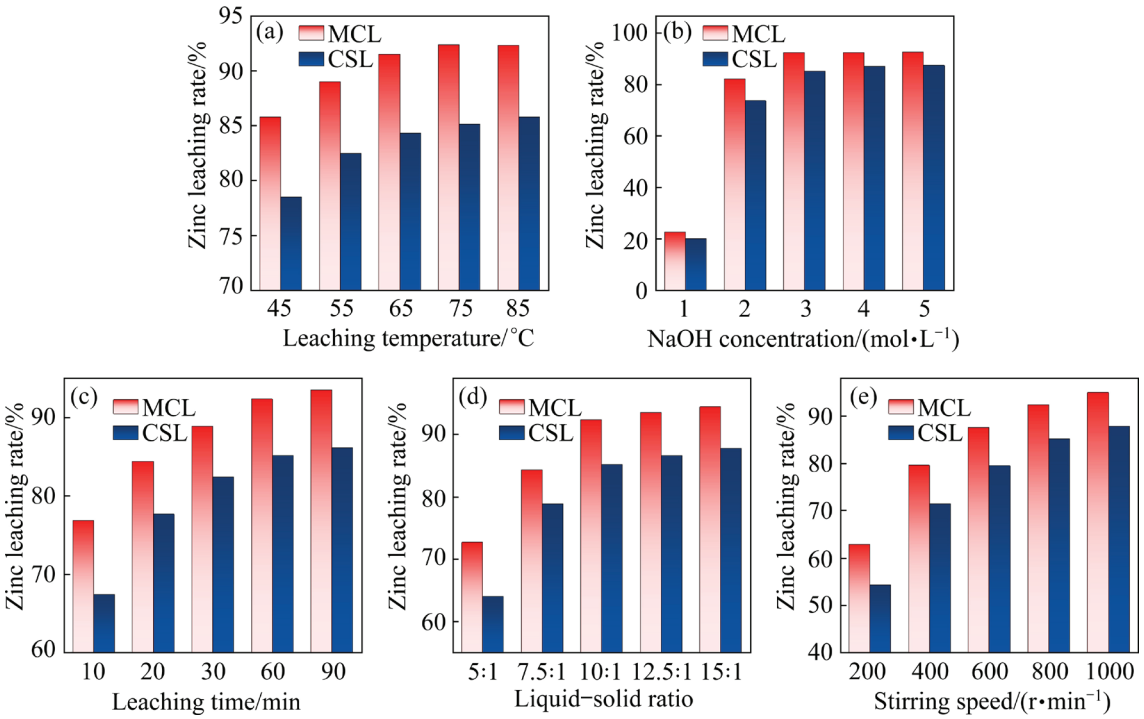

Fig. 4 Effects of different leaching conditions on zinc leaching rate: (a) Leaching temperature; (b) NaOH concentration; (c) Leaching time; (d) Liquid–solid ratio; (e) Stirring speed

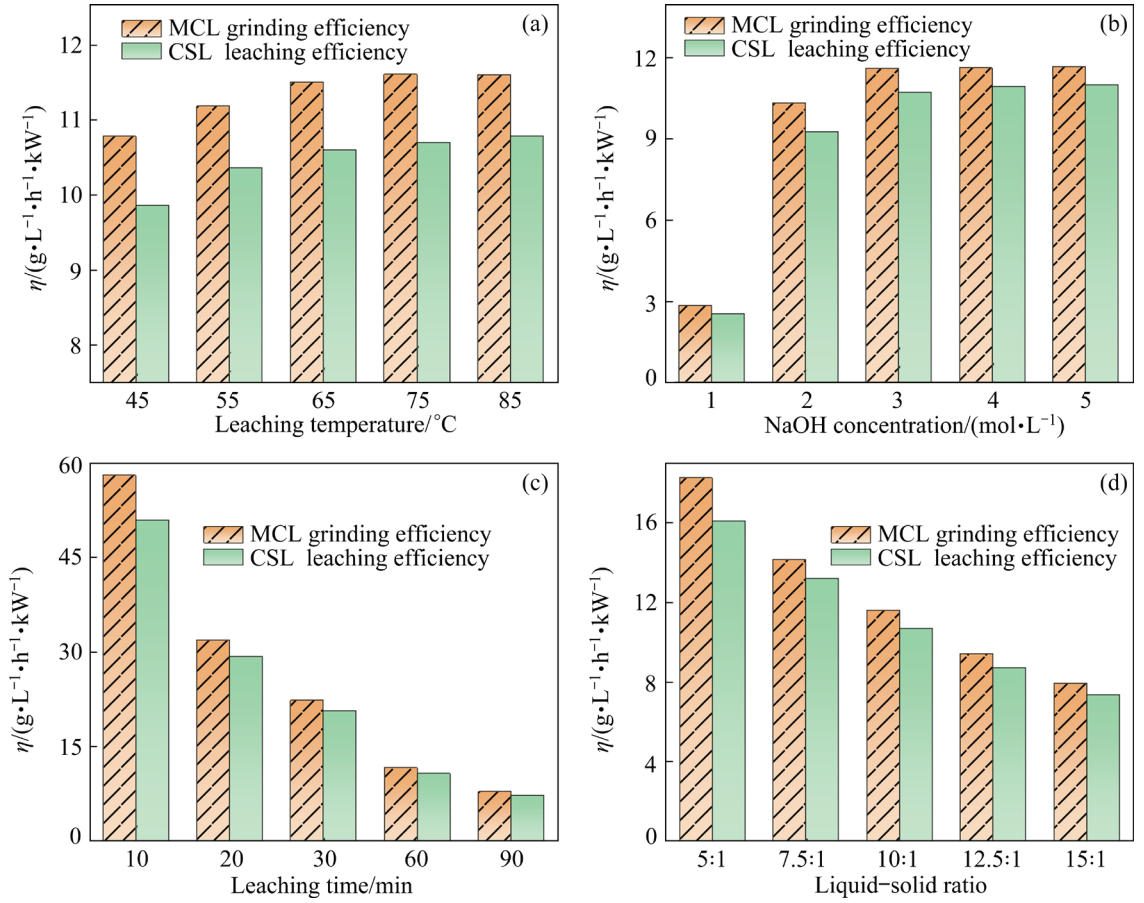

Fig. 5 Effects of different leaching conditions on zinc extraction efficiency: (a) Leaching temperature; (b) NaOH concentration; (c) Leaching time; (d) Liquid–solid ratio

3.1 Effect of leaching temperature

Temperature is a key factor affecting leaching. According to leaching kinetics, an increase in temperature can accelerate the leaching reaction rate, which is beneficial to easily reaching chemical reaction balance. A comparative study on the effect of leaching temperature on zinc leaching was carried out under MCL and CSL. XRD analysis of leaching residue was also performed to investigate the effect of leaching temperature on the leaching of lead–zinc oxide ores (Fig. 6).

The experiment was conducted under the following conditions: NaOH concentration of 3 mol/L, leaching time of 60 min, liquid–solid ratio of 10∶1, and stirring speed of 800 r/min. Figure 4(a) shows the comparative study of the effects of MCL and CSL on the zinc leaching rate at different leaching temperatures. In MCL and CSL, the zinc leaching rate increased with the increase of temperature. MCL was always better than CSL. With the increasing temperature, the grinding efficiency of MCL and the leaching efficiency of CSL both increased (Fig. 5(a)). Compared with CSL, MCL reduced the reaction temperature to achieve the same zinc extraction effect as CSL. When the temperature was continuously increased to 85 °C, the zinc leaching rate under MCL remained unchanged but that under CSL continued to increase at a slow rate. This phenomenon occurred because chemical reaction equilibrium was attained at 85 °C in MCL but not in CSL. The energy consumption must be correspondingly increased when the temperature was increased. In conclusion, the optimal leaching temperature was set to be 75 °C.

The phase types of MCLR and conventional stirring leaching residue (CSLR) were the same at different temperatures (Figs. 6(a) and (b)) and were mainly composed of calcite, quartz, galena, and magnetite. Smithsonite and cerussite in the raw ores disappeared, which was consistent with the high zinc leaching rate. The main reaction equations during leaching can be described by Eqs. (4) and (5). With the XRD data as basis, the A and FWHM were investigated with the strongest peak of leaching residue, that is, the main peak of calcite phase. With increasing the temperature, the peak intensity of MCLR and CSLR showed a downward

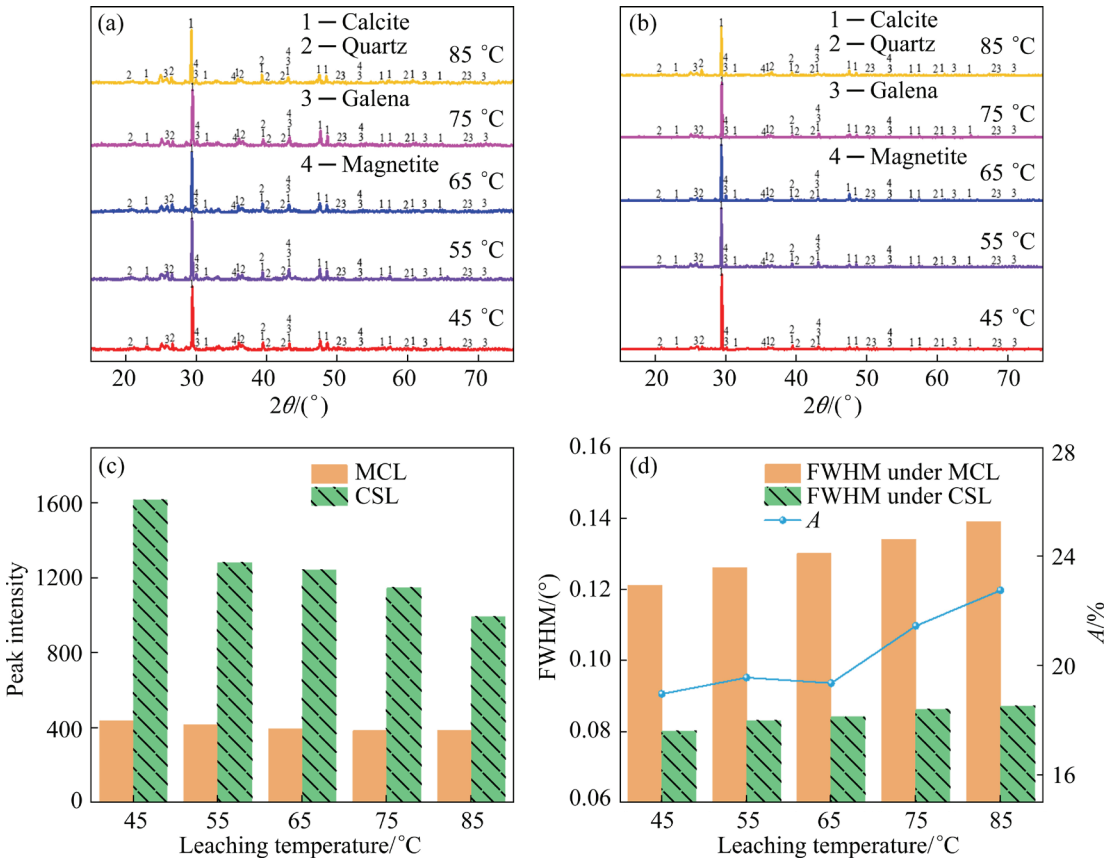

Fig. 6 XRD patterns of alkali leaching residue at different temperatures: (a) MCLR; (b) CSLR; Comparison chart of alkali leaching residue data at different temperatures: (c) Peak intensity; (d) FWHM and amorphization degree (A)

trend and was lower in the former (Fig. 6(c)). With increasing the temperature, the FWHM increased in MCLR and CSLR and was greater in the former than in the latter. Moreover, the A of MCLR showed an upward trend overall (Fig. 6(d)). Increasing temperature can accelerate the mass transfer rate of the solution, induce the reaction between the solution and minerals, and strengthen the dissolution effect of zinc-containing components. Compared with the conventional process, mechanochemical activation can refine lead–zinc oxide mineral particles, destroy the grain integrity, produce lattice distortion, and increase the degree of amorphization, thereby improving the zinc leaching rate.

$$ZnCO_3+4NaOH=Na_2Zn(OH)_4+Na_2CO_3 \quad (4)$$

$$PbCO_3+4NaOH=Na_2Pb(OH)_4+Na_2CO_3 \quad (5)$$

3.2 Effect of NaOH concentration

A comparative study on the effect of NaOH concentration on zinc leaching was carried out under MCL and CSL. XRD analysis of the leaching residue was also performed to investigate the effect of NaOH concentration on the leaching of lead–zinc oxide ores (Fig. 7). The experiment was conducted under the following conditions: leaching temperature of 75 °C, leaching time of 60 min, liquid–solid ratio of 10:1, and stirring speed of 800 r/min. With increasing the NaOH concentration, the change trend of zinc leaching rate was similar between MCL and CSL, but the former was always better than the latter (Fig. 4(b)). When the concentration of NaOH was increased from 1 to 5 mol/L, the zinc leaching rate increased, but the increase rate gradually decreased. With increasing the NaOH concentration, the grinding efficiency of MCL and the leaching efficiency of CSL were similar, that is, they both increased but the increase rate gradually decreased (Fig. 5(b)). MCL reduced the NaOH concentration to achieve the same zinc extraction effect as CSL. When the NaOH concentration reached 3 mol/L, the zinc leaching rate under MCL was 92.3%, and that under CSL was 85.1%. When the NaOH concentration was further increased to 5 mol/L, the zinc leaching rate only slightly increased.

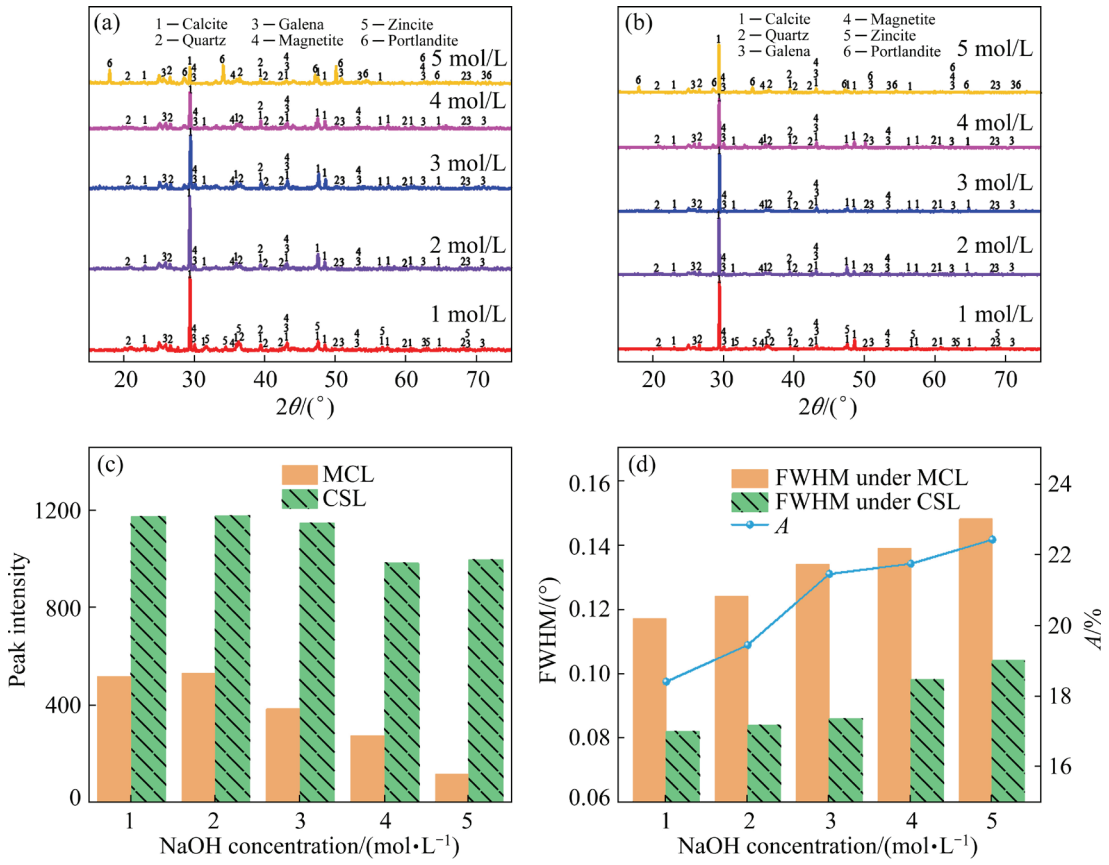

Fig. 7 XRD patterns of alkali leaching residue at different NaOH concentrations: (a) MCLR; (b) CSLR; Comparison charts of alkali leaching residue data at different NaOH concentrations: (c) Peak intensity; (d) FWHM and amorphization degree (A)

Hence, the optimal alkalinity level was 3 mol/L NaOH.

When the NaOH concentration was 1 mol/L, the XRD patterns of MCLR and CSLR in Figs. 7(a) and (b) showed the zincite phase and the disappearance of the smithsonite phase in the raw ores. According to the low zinc leaching rate (Fig. 4(b)), NaOH at this concentration was insufficient to completely dissolve zinc in minerals. Hence, the reaction of Eq. (6) may occur. With further increase in NaOH concentration, the zincite phase in the leaching residue disappeared. When the concentration of NaOH was sufficient, the soluble zinc components in the raw ores were almost completely dissolved and entered the alkali solution to form sodium zincate. When the concentration of NaOH was continuously increased to 5 mol/L, the XRD spectra of MCLR and CSLR showed the portlandite phase. At extremely high NaOH concentration, the solubility of $CaCO_3$ was greater than that of $Ca(OH)_2$, and the solid phase structure of calcite was unstable [29]. In this regard, reversed causticizing reaction may occur as indicated in Eq. (7). With increasing the NaOH concentration, the peak intensity of MCLR and CSLR decreased, and the FWHM of MCLR and CSLR increased (Figs. 7(c) and (d)). Increasing the NaOH concentration can improve the leaching rate because high-concentration solutions are more likely to damage minerals; MCL intensifies the damage effect of raw ore through mechanochemical activation, resulting in the decreased diffraction peak intensity of the leaching residue and FWHM broadening [15,28]. The degree of amorphization was intensified to be evident in the A of MCLR (Figs. 7(c) and (d)). In terms of macro performance, the leaching residue particles were more delicate, thereby strengthening the zinc leaching effect.

$$ZnCO_3+NaOH=ZnO+NaHCO_3 \quad (6)$$

$$CaCO_3+2NaOH \rightleftharpoons Ca(OH)_2 + Na_2CO_3 \quad (7)$$

3.3 Effect of leaching time

A comparative study on the effect of MCL and CSL on zinc leaching at different leaching time, and the XRD analysis of leaching residue were carried out (Fig. 8). The experiment was conducted under the following conditions: NaOH concentration of

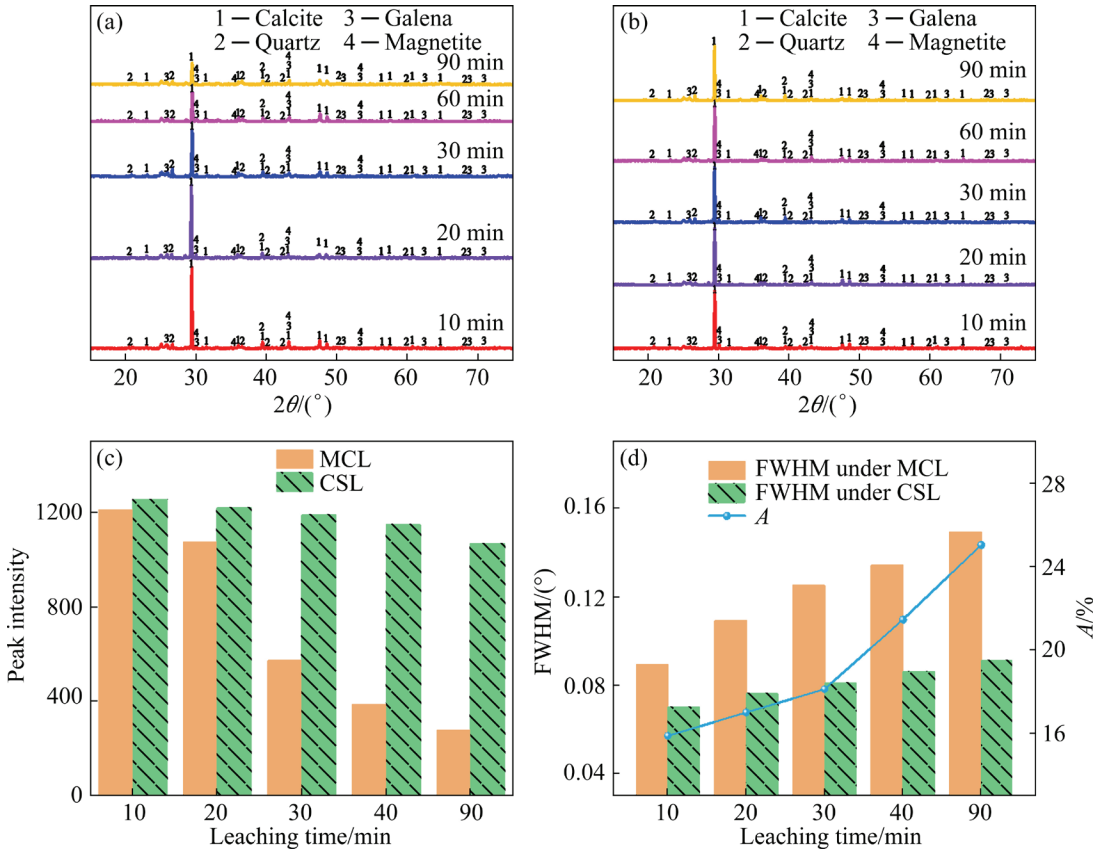

Fig. 8 XRD patterns of alkali leaching residue at different leaching time: (a) MCLR; (b) CSLR; Comparison charts of alkali leaching residue data at different leaching time: (c) Peak intensity; (d) FWHM and amorphization degree (A)

3 mol/L, leaching temperature of 75 °C, liquid–solid ratio of 10:1, and stirring speed of 800 r/min.

The zinc leaching rate increased with increasing the leaching time in both methods, but MCL was better than CSL because soluble zinc can be leached in a short time (Fig. 4(c)). The grinding efficiency of MCL and the leaching efficiency of CSL (Fig. 5(c)) exhibited a sharp downward trend with further increase in leaching time. From 10 to 90 min, the grinding efficiency decreased sharply from 57.99 to 7.84 g/(L·h·kW) under MCL, and the leaching efficiency decreased from 50.86 to 7.22 g/(L·h·kW) under CSL. The reaction rate of NaOH for leaching zinc was fast in the initial stage and mainly controlled by diffusion in the later stage. Extending the leaching time for zinc extraction is of minimal significance and will increase the production cost. MCL shortened the leaching time to achieve the same zinc extraction effect as CSL. The residue phase of the leaching residue mainly consisted of gangue and insoluble metals (Figs. 8(a) and (b)). With increasing the leaching time, the diffraction peak intensity of MCLR and CSLR decreased and the FWHM increased; however, the change trend of CSLR was not as evident as that of MCLR, and the A of MCLR increased (Figs. 8(c) and (d)). MCL destroyed the insoluble gangue layer on the surface of zinc ore by simultaneous grinding and leaching, accelerated the exposure of internal zinc containing components and the reduction in particle size, and strengthened the zinc dissolution effect of NaOH. In consideration of the leaching rate and production cost, the optimal leaching time was set to be 60 min.

3.4 Effect of liquid–solid ratio

A comparative study on the effect of liquid–solid ratio on zinc leaching was carried out under MCL and CSL. XRD analysis was also conducted on the leached residue to determine the influence of liquid–solid ratio on raw ore leaching (Fig. 9). The experiment was conducted under the following conditions: NaOH concentration of 3 mol/L, leaching temperature of 75 °C, leaching time of 60 min, and stirring speed of 800 r/min. The zinc leaching rate and liquid–solid ratio of zinc leaching showed the

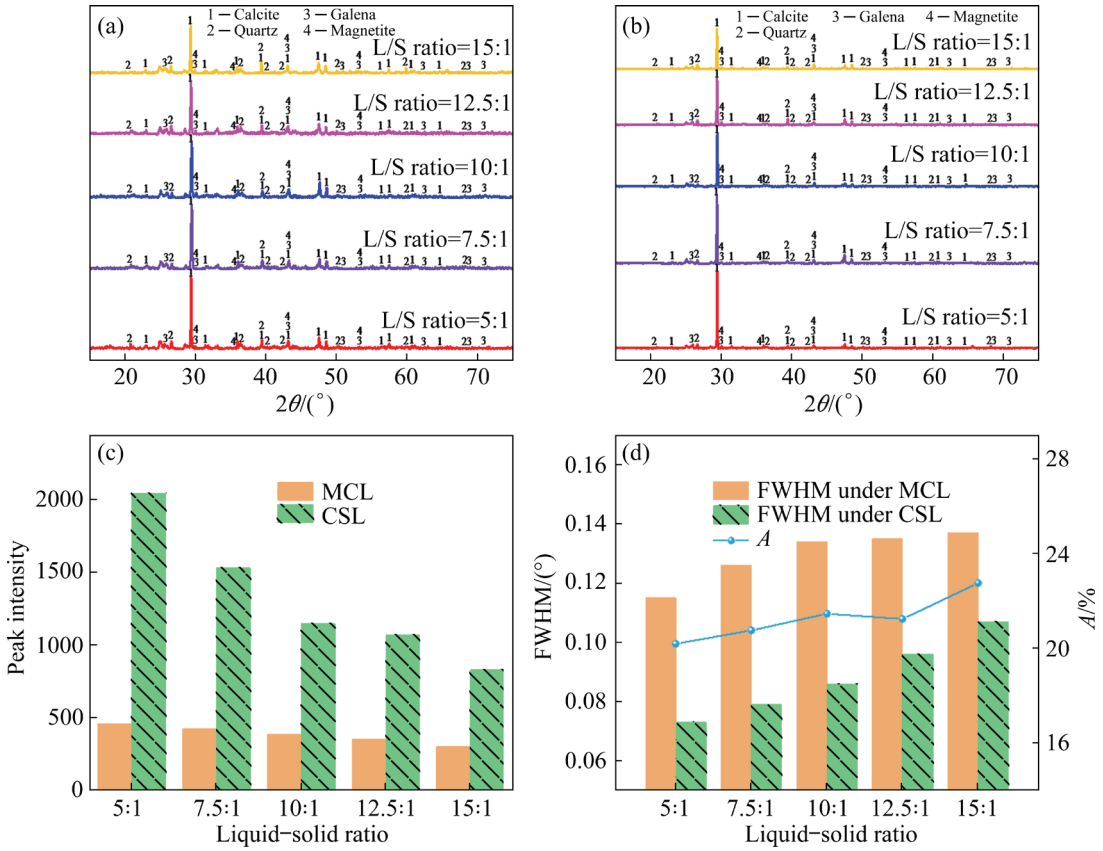

Fig. 9 XRD patterns of alkali leaching residue at different liquid–solid (L/S) ratios: (a) MCLR; (b) CSLR; Comparison charts of alkali leaching residue data at different liquid–solid ratio: (c) Peak intensity; (d) FWHM and amorphization degree (A)

same trend in both methods, that is, the zinc leaching rate increased with increasing the liquid–solid ratio. However, MCL was always better than CSL (Fig. 4(d)). With increasing the liquid–solid ratio, the grinding efficiency of MCL and the leaching efficiency of CSL both showed a downward trend (Fig. 5(d)). When the liquid–solid ratio was 5∶1, the zinc leaching rate in MCL was 72.7%, and the grinding efficiency of MCL was 18.27 g/(L·h·kW). The zinc leaching rate in CSL was 64.0%, and the CSL leaching efficiency was 16.09 g/(L·h·kW). When the liquid–solid ratio was continuously increased to 10∶1, the zinc leaching rate increased to 92.3% under MCL and 85.1% under CSL. However, the grinding efficiency of MCL decreased to 11.61 g/(L·h·kW), and the leaching efficiency of CSL decreased to 10.70 g/(L·h·kW). With further increase in the liquid–solid ratio to 15∶1, the zinc leaching rate of both methods slightly increased and their zinc extraction efficiency were further reduced. In consideration of NaOH solution consumption, zinc extraction efficiency, and zinc leaching rate, the optimal liquid–solid ratio was set to be 10∶1.

No difference in phase types, mainly calcite, quartz, galena, and magnetite, was found between MCLR and CSLR at different liquid–solid ratios (Figs. 9(a) and (b)). With increasing the liquid–solid ratio, the peak strengths of MCLR and CSLR showed a downward trend. The peak strengths of MCLR did not decline significantly but were lower than those of CSLR (Fig. 9(c)). With increasing the liquid–solid ratio, the A of MCLR showed an increasing trend, the FWHM of MCLR and CSLR also increased, and the FWHM of MCLR was always greater than that of CSLR (Fig. 9(d)). Increasing the liquid–solid ratio also increased the contact probability between zinc ore and NaOH solution, reduced the mass transfer diffusion resistance, and promoted the dissolution of zinc. MCL intensified the destruction of zinc ore particles by mechanochemical activation, leading to a reduction in particle size and intensification of amorphization. This phenomenon promoted the increase in the mass transfer rate, improved the zinc leaching rate, and reduced the liquid–solid ratio, thereby achieving the same zinc leaching effect as CSL.

3.5 Effect of stirring speed

A comparative study on the effect of MCL and CSL on zinc leaching rate at different stirring speeds, and XRD analysis of leaching residue were carried out (Fig. 10). The experiment was conducted under the following conditions: NaOH concentration of 3 mol/L, leaching temperature of 75 °C, leaching time of 60 min, and liquid–solid ratio of 10∶1.

Under MCL and CSL, the zinc leaching rate was basically consistent with the change trend of stirring speed. At a low rotating speed, the zinc leaching rate was also low. Increasing the rotating speed also increased the zinc leaching rate, and MCL was better than CSL (Fig. 4(e)). The XRD phases of MCLR and CSLR were mainly insoluble metals and gangue (Figs. 10(a) and (b)). The grinding efficiency of MCL and the leaching efficiency of CSL were not studied due to different levels of working power of basket grinder at different stirring speeds. Increasing the stirring speed led to the complete mixing and dispersal of the zinc ore powder in the NaOH solution system, thereby thinning out the particle surface diffusion layer, expanding the mass transfer rate, and increasing the zinc leaching rate. However, increasing the stirring speed also increased the energy consumption. With increasing the stirring rate, the diffraction peak intensity of MCLR and CSLR decreased, and the FWHM increased. The peak intensity of MCLR and CSLR was almost the same at 800 and 1000 r/min, respectively, the FWHM broadening change in CSLR was not evident, and the A of MCLR continued to increase (Figs. 10(c) and (d)). Increasing the stirring speed also accelerated the solution dissolution of ores. Meanwhile, MCL dissolved the zinc ores by grinding and leaching, accelerated the exposure of internal zinc-containing components and particle amorphization, and strengthened the zinc leaching effect. In consideration of the leaching rate and energy consumption, the optimal stirring speed was set to be 800 r/min.

The optimal technological conditions for the alkaline leaching of low-grade lead–zinc oxide ores under MCL were as follows: leaching temperature of 75 °C, NaOH concentration of 3 mol/L, leaching time of 60 min, liquid–solid ratio of 10:1, and stirring speed of 800 r/min. Under these conditions, the zinc leaching rate reached 92.3%. Compared with CSL, MCL enhanced the zinc leaching effect and reduced the reaction conditions. Therefore, MCL could be superior to CSL.

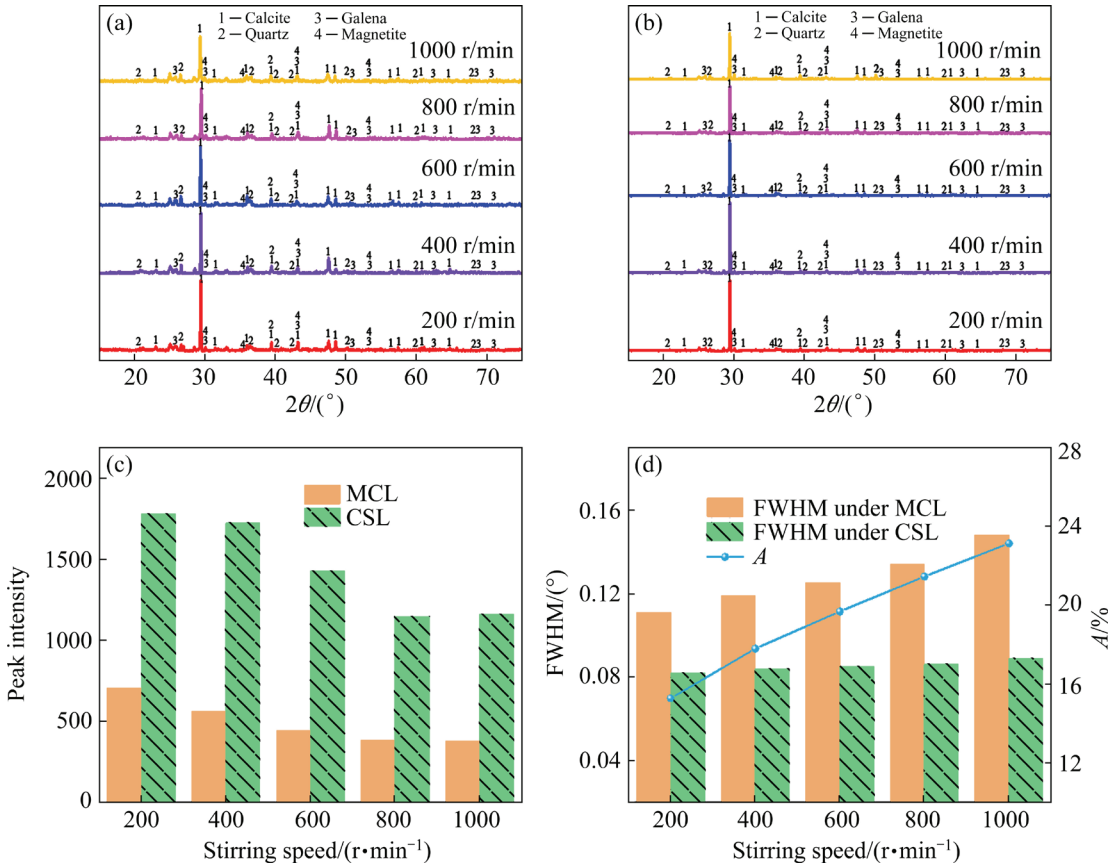

Fig. 10 XRD patterns of alkali leaching residue at different stirring speeds: (a) MCLR; (b) CSLR; Comparison charts of alkali leaching residue data at different stirring speeds: (c) Peak intensity; (d) FWHM and amorphization degree (A)

3.6 Enhancement mechanism of MCL

Figure 11 shows the measured energy consumption of MCL and CSL under the optimal condition, indicating that the difference between them was not significant. The leaching residues treated by MCL and CSL under the optimal experimental conditions were characterized and analyzed, as shown in Fig. 12. Figure 12(a) shows the comparative XRD diagram of MCLR and CSLR. The two leaching residues had the same composition, mainly including gangue components of calcite, quartz and small amount of galena and magnetite, but no smithsonite and cerussite. For the diffraction peak of calcite, its main peak intensity in MCLR was smaller than that in CSLR. Hence, MCL can effectively leach the soluble zinc in lead–zinc oxide ores, reduce the crystallinity of minerals, and destroy the crystal structure of minerals to dissolve some gangue components. From a macroscopic perspective, MCLR is light in color and the particles are fine without graininess. Meanwhile, CSLR is dark in color and the particles are rough with graininess (Fig. 12(b)). In terms of microstructure, the particle size distribution curve of MCLR moved to the left, the fine particle size distribution increased, and the coarse particle size distribution decreased compared with those in CSLR. These findings showed that the overall particle size of the leached residue gradually shrank (Figs. 12(c) and (d)). The specific granularity data are shown in Table 4.

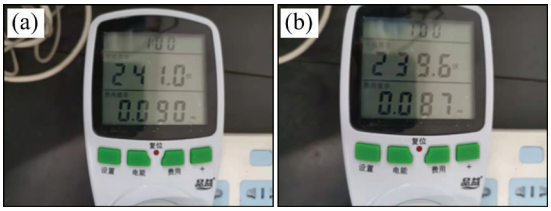

Fig. 11 Energy consumption of different leaching processes: (a) MCL; (b) CSL

SEM characterization was carried out for MCLR and CSLR to evaluate changes in the leaching residues (Fig. 13). Microanalysis of the leaching residue was also conducted through EDS (Table 5). Coarse and smooth particles appeared in

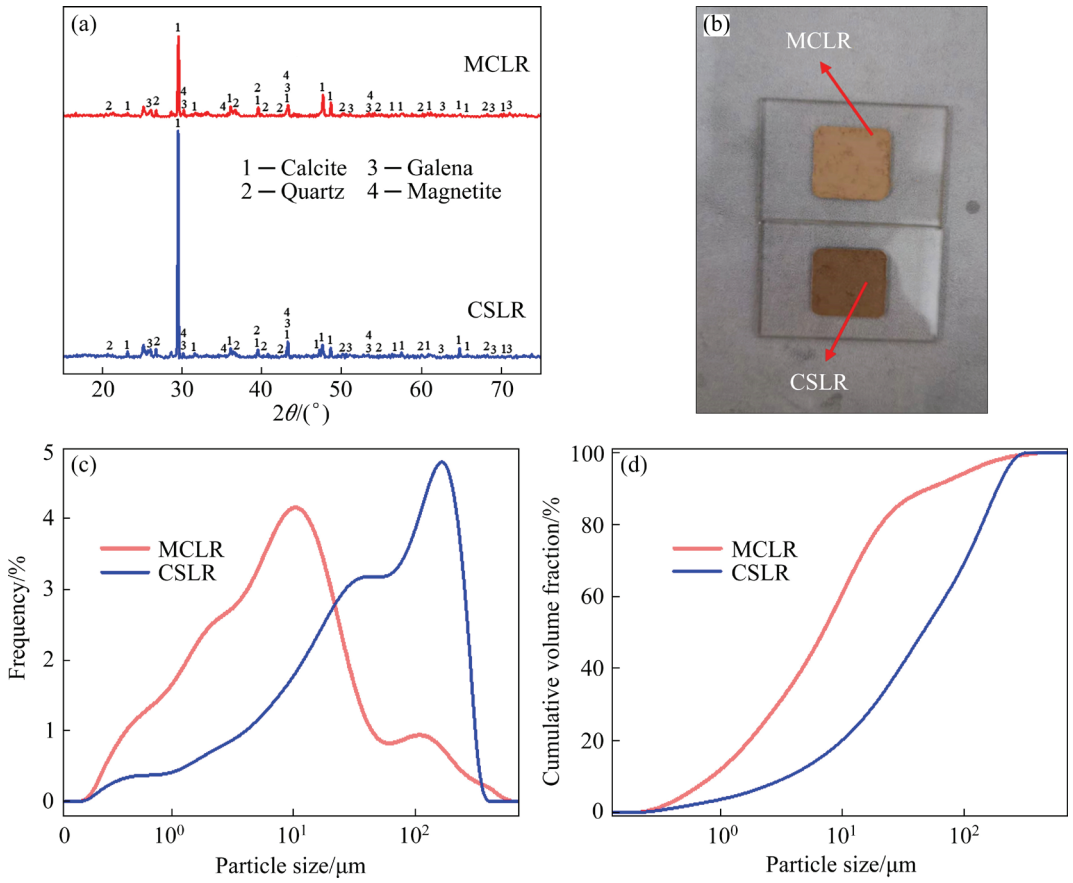

Fig. 12 Comparison diagrams of related characterization of leaching residue under different leaching processes: (a) XRD patterns; (b) Physical diagram; (c) Particle size distribution; (d) Cumulative particle size distribution

Table 4 Particle size distribution and specific surface area of MCLR and CSLR samples

Sample	D_{10}/ μm	D_{50}/ μm	D_{90}/ μm	$D_{3,2}$/ μm	$D_{4,3}$/ μm	S_G/ ($m^2 \cdot g^{-1}$)
MCLR	0.855	6.908	50.48	2.39	21.669	2.51
CSLR	3.61	45.47	185.125	6.831	73.016	0.878

Table 5 Contents of main elements in selected areas in EDS analysis results of MCLR and CSLR samples in Fig. 13 (wt.%)

Element	Point No.							
	1	2	3	4	5	6	7	8
C	53.98	29.73	20.68	12.92	11.99	21.91	5.74	11.43
O	28.65	4.4	47	47.34	55.6	37.77	24.94	46.9
Si	–	0.08	0.25	0.07	–	–	0.32	–
S	0.59	18.99	0.5	0.26	1.43	5.06	0.23	2.43
Ca	6.31	0.73	17.93	37.92	16.19	9.15	0.16	26.87
Fe	4.73	1.07	9.18	0.42	1.75	12.29	68.3	5.51
Zn	0.74	43.72	1.82	0.52	3.92	7.06	0.31	3.15
Pb	5.02	1.28	2.23	0.55	9.14	6.77	–	3.72

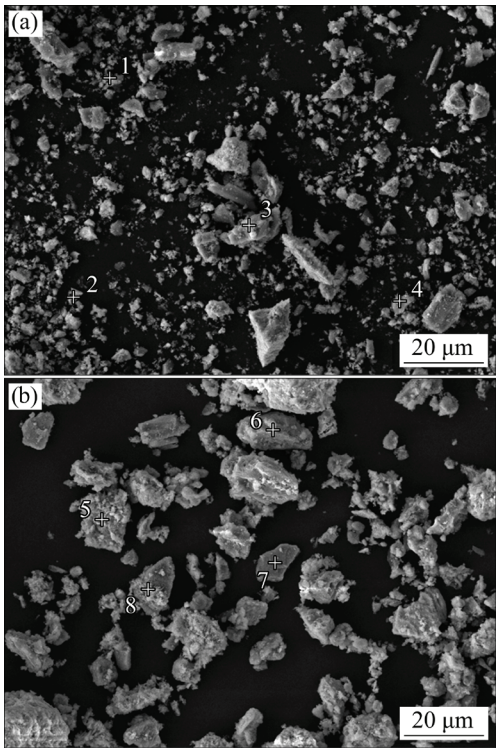

Fig. 13 SEM images of different leaching residues: (a) MCLR; (b) CSLR

the microstructure of the two leaching residues, but the particle size was small for MCLR and large for CSLR. EDS analysis showed that the Zn content in MCLR was lower than that in CSLR. However, the Zn and S contents at Point 2 of MCLR were extremely high, indicating that these two elements existed in the form of ZnS. However, the element content of EDS was not accurate and can only be used for reference [30]. EPMA was conducted to further analyze the element distribution of MCLR and CSLR, as shown in Fig. 14. The main elements in the leaching residue were Ca, C, Si, and O, indicating that the main residue phases were the gangue components of $CaCO_3$ and SiO_2. This

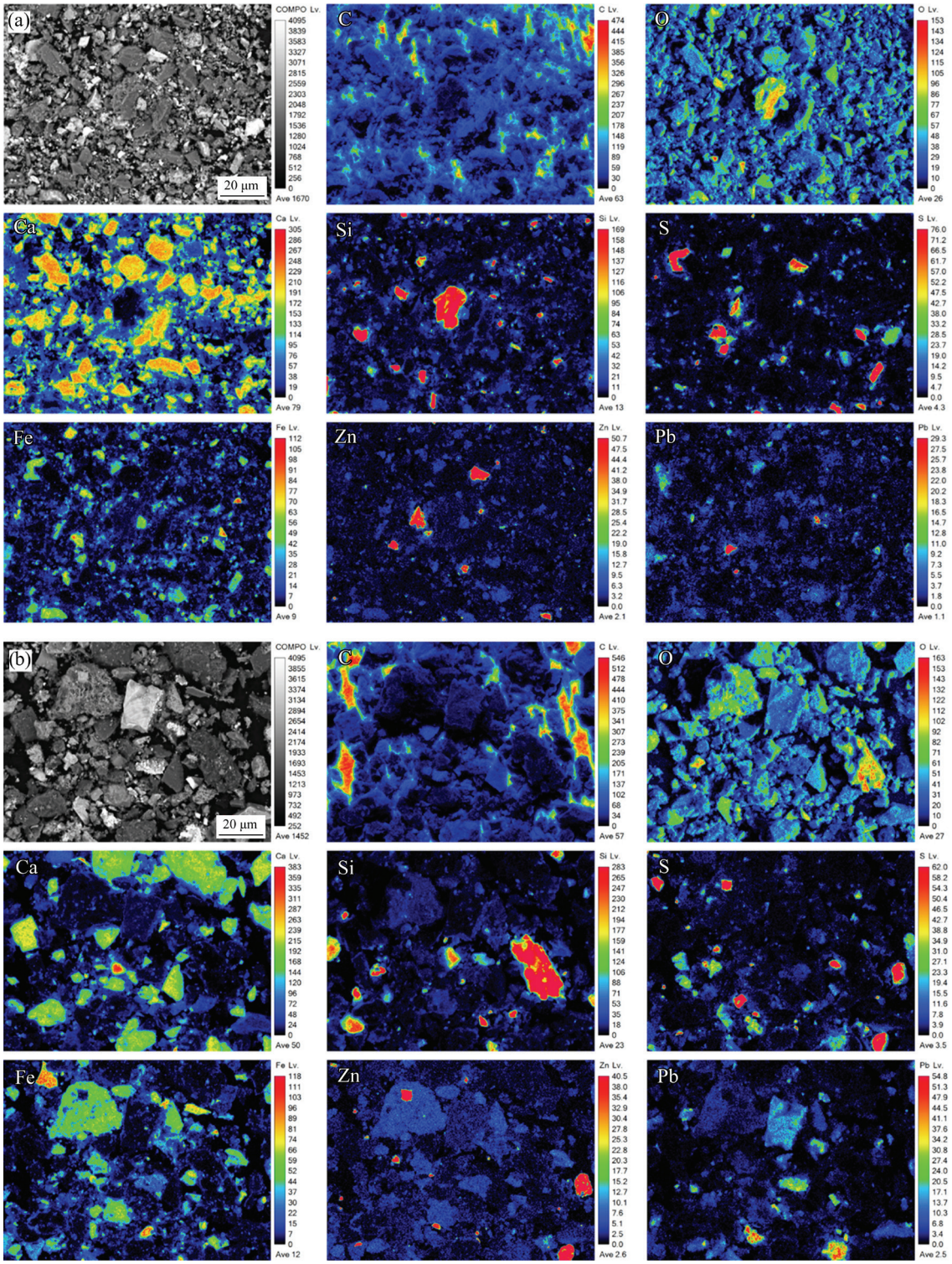

Fig. 14 EPMA images of different leaching residues: (a) MCLR; (b) CSLR

finding was consistent with the XRD results. Small amounts of Zn, Pb, Fe, and S remained in the leaching residue particles. The distribution of Pb overlapped with those of Fe, S, O, and other elements, and Zn is mainly combined with Fe, S and O. This finding indicated that plumbum existed in the form of PbS and oxides. In addition, small amounts of zinc-containing minerals in the leaching residue existed in the form of hard soluble zinc, such as ZnS and $ZnFe_2O_4$, and the content of Zn was low in MCLR.

Table 2 showed that $ZnCO_3$ phase accounted for 85.58% of the lead–zinc oxide ores, alkali soluble zinc accounted for 90.07%, and refractory zinc phase accounted for 9.93%. The zinc leaching rate of MCL and CSL was increased by improving the reaction conditions as shown in Fig. 15. According to the characteristics of Zn—S and Zn—O bonds [31−33], the decreasing active order of zinc-containing phase in alkaline solution system is: $ZnCO_3$ > ZnO > Zn_2SiO_4 > ZnS > $ZnFe_2O_4$. For CSL, improving the reaction conditions can completely leach $ZnCO_3$, but the zinc leaching rate is always lower than the alkali soluble zinc rate and the refractory zinc phase is difficult to leach by using NaOH solution under the conventional process. However, Fig. 15 showed that the zinc leaching rate under MCL was higher than the alkali soluble zinc rate. This finding indicates that mechanochemical activation dissolves some zinc components that are difficult to leach. Given that $ZnFe_2O_4$ is difficult to leach in NaOH solution, ZHANG et al [23,34,35] used NaOH solution containing lead carbonate to leach fluorescent zinc sulfide and sphalerite under the condition of mechanical activation and achieved relatively good zinc leaching effect. Therefore, ZnS is the phase of zinc that is difficult to leach, which is leached in MCL and may cause the reaction of Eq. (8):

$$ZnS+PbCO_3+4NaOH=Na_2Zn(OH)_4+PbS+Na_2CO_3 \quad (8)$$

Given that cerussite already exists in the raw ore composition, the zinc leaching effect can be enhanced without introducing additional $PbCO_3$ to react with ZnS in MCL. The leaching mechanisms of MCL and CSL according to the leaching experiment results and characterization analysis are shown in Fig. 16. In CSL, with NaOH solution at appropriate concentration, OH^- breaks through the solid particles of lead−zinc oxide ore to reach the reaction core, reacts with $ZnCO_3$ and $PbCO_3$, and generates $Zn(OH)_4^{2-}$ and $Pb(OH)_4^{2-}$ into the solution. Owing to the different solubilities of ZnS and PbS, adding an appropriate amount of Na_2S solution is necessary to produce Pb prior to Zn precipitation to

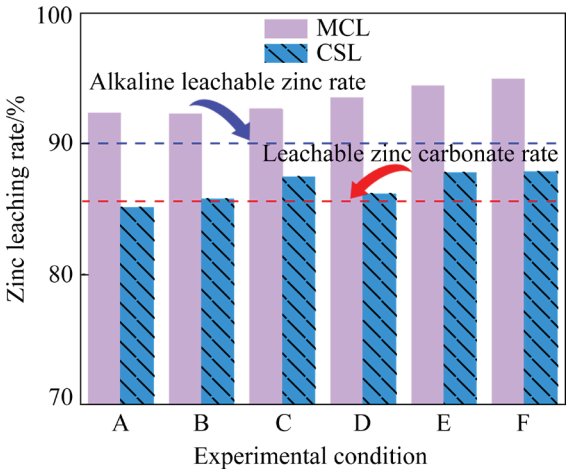

Fig. 15 Effect of different experimental conditions on zinc leaching rate: A−75 °C, 3 mol/L NaOH, 60 min, L/S ratio=10:1 and 800 r/min; B−85 °C, 3 mol/L NaOH, 60 min, L/S ratio=10:1 and 800 r/min; C−75 °C, 5 mol/L NaOH, 60 min, L/S ratio=10:1 and 800 r/min; D−75 °C, 3 mol/L NaOH, 90 min, L/S ratio=10:1 and 800 r/min; E−75 °C, 3 mol/L NaOH, 60 min, L/S ratio=15:1 and 800 r/min; F−75 °C, 3 mol/L NaOH, 60 min, L/S ratio=10:1 and 1000 r/min

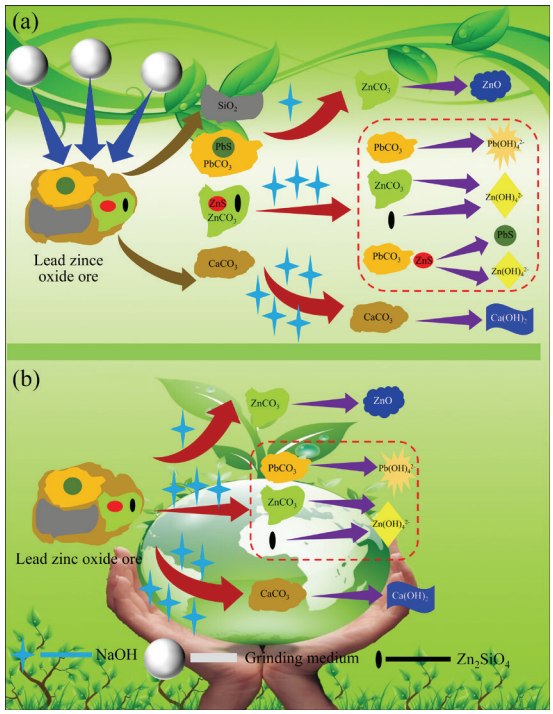

Fig. 16 Schematic diagrams showing leaching mechanism of MCL (a) and CSL (b)

generate PbS. Meanwhile, Zn still exists in the alkaline solution in the form of ions to separate lead from zinc and recover lead from PbS precipitation according to Refs. [36−38]. When the concentration of NaOH is insufficient, it will react with $ZnCO_3$ and generate ZnO in the solid particle product layer. When the concentration of NaOH is excessive, it will react with $CaCO_3$ in the raw ore and generate $Ca(OH)_2$ in the solid product layer on the basis of leaching $Zn(OH)_4^{2-}$ and $Pb(OH)_4^{2-}$. Finally, the mechanisms underlying the mechano-chemical activation of MCL are presented as follows [11−13,39,40]: (1) Change the physical properties of mineral particles, destroy the surface of solid during the leaching, open the mineral inclusions and refine the particles, release the Zn and Pb, and increase the mass transfer rate, thus strengthen the zinc leaching; (2) Change the microstructure of mineral particles, resulting in crystal structure defects, such as reduced diffraction peak strength, FWHM broadening, and increased amorphization, storing and converting part of mechanical energy into chemical energy, thereby improving the reactivity of materials [39,40]; (3) Change the chemical properties of mineral particles to reduce the dependence of leaching reaction on leaching temperature and concentration of leaching agent, and realize the chemical reaction that is difficult to occur under the conventional process to dissolve the refractory zinc components and improve the zinc leaching rate [23,39].

4 Conclusions

(1) Compared with CSL, MCL can shorten the leaching time, reduce the reaction conditions, and enhance the zinc leaching effect of NaOH by destroying the mineral particle structure during grinding while leaching. The optimal leaching conditions were as follows: leaching temperature of 75 °C, NaOH concentration of 3 mol/L, leaching time of 60 min, liquid–solid ratio of 10∶1, and stirring speed of 800 r/min. Under these optimal conditions, the zinc leaching rate was 92.3%, which was 7.2% higher than that in CSL.

(2) The energy consumption of the leaching process was studied under the optimal leaching conditions. Characterization analysis (XRD, SEM–EDS, particle size analysis, and EPMA) for the leached residue and zinc phase analysis of the raw ore were carried out. The XRD data were analyzed (peak intensity, FWHM and amorphization degree *A*). The results showed that the residual zinc-containing components in the leaching residue have difficulty leaching zinc phases such as ZnS and $ZnFe_2O_4$. On this basis, the strengthening mechanism of mechanochemical activation was studied.

(3) MCL can effectively extract zinc under the condition of low energy consumption, and the NaOH solution after leaching can be recycled. Thus, this method causes no pollution to the environment and has a promising industrial prospect. A practical reference scheme is provided to solve the problem of resource utilization for low-grade refractory lead–zinc oxide ores in the Lanping area. Further optimization of equipment configuration can be beneficial to the industrial application and promotion of MCL in the future.

CRediT authorship contribution statement

Yu-sen YU: Conceptualization, Data curation, Formal analysis, Investigation, Methodology, Writing − Original draft, Writing − Review and editing; **Li-xue CUI:** Validation, Data curation, Investigation, Visualization; **Li-bo ZHANG:** Conceptualization, Funding acquisition, Resources, Supervision, Validation; **Yun-fan WANG:** Conceptualization, Funding acquisition, Resources, Validation, Methodology, Writing − Review and editing, Supervision.

Declaration of competing interest

The authors declare that they have no known competing financial interests or personal relationships that could have appeared to influence the work reported in this paper.

Acknowledgments

The authors are grateful for the financial supports from the National Natural Science Foundation of China (No. 52264030), the Yunnan Fundamental Research Projects, China (No. 202201BE070001-048), and the Special Fund Projects of Central Government Guiding Local Science and Technology Development, China (No. 202107AA110002).

References

[1] LIU Zhi-yong, LIU Zhi-hong, LI Qi-hou, YANG Tian-zu, ZHANG Xu. Leaching of hemimorphite in NH_3–$(NH_4)_2SO_4$–H_2O system and its mechanism [J]. Hydrometallurgy, 2012, 125/126: 137−143.

[2] XU Hong-sheng, WEI Chang, LI Chu-xiong, FAN Gang, DENG Zhi-gan, ZHOU Xue-jiao, QIU Shuang. Leaching of a complex sulfidic, silicate-containing zinc ore in sulfuric acid solution under oxygen pressure [J]. Separation and Purification Technology, 2012, 85: 206−212.

[3] YANG Tian-zu, RAO Shuai, ZHANG Du-chao, WEN Jian-feng, LIU Wei-feng, CHEN Lin, ZHANG Xin-wang. Leaching of low grade zinc oxide ores in nitrilotriacetic acid solutions [J]. Hydrometallurgy, 2016, 161: 107−111.

[4] ABKHOSHK E, JORJANI E, AL-HARAHSHEH M S, RASHCHI F, NAAZERI M. Review of the hydrometallurgical processing of non-sulfide zinc ores [J]. Hydrometallurgy, 2014, 149: 153−167.

[5] XU Hong-sheng, WEI Chang, LI Cun-xiong, FAN Gang, DENG Zhi-gan, LI Min-ting, LI Xing-bin. Sulfuric acid leaching of zinc silicate ore under pressure [J]. Hydrometallurgy, 2010, 105(1/2): 186−190.

[6] FRENAY J. Leaching of oxidized zinc ores in various media [J]. Hydrometallurgy, 1985, 15(2): 243−253.

[7] CHEN Ai-liang, ZHAO Zhong-wei, JIA Xi-jun, LONG Shuang, HUO Guang-sheng, CHEN Xing-yu. Alkaline leaching Zn and its concomitant metals from refractory hemimorphite zinc oxide ore [J]. Hydrometallurgy, 2009, 97(3/4): 228−232.

[8] YUAN Tie-chui, CAO Qin-yuan, LI Jie. Effects of mechanical activation on physicochemical properties and alkaline leaching of hemimorphite [J]. Hydrometallurgy, 2010, 104(2): 136−141.

[9] DHAWAN N, SAFARZADEH M S, BIRINCI M. Kinetics of hydrochloric acid leaching of smithsonite [J]. Russian Journal of Non-Ferrous Metals, 2011, 52(3): 209−216.

[10] SANTOS F M F, PINA P S, PORCARO R, OLIVEIRA V A, SILVA C A, LEAO V A. The kinetics of zinc silicate leaching in sodium hydroxide [J]. Hydrometallurgy, 2010, 102(1/2/3/4): 43−49.

[11] BALAZ P. Mechanochemistry in nanoscience and minerals engineering [M]. Heidelberg: Springer-Verlag, 2008.

[12] GUO Xiu-ying, XIANG Dong, DUAN Guang-hong, MOU Peng. A review of mechanochemistry applications in waste management [J]. Waste Management, 2010, 30(1): 4−10.

[13] BALAZ P. Mechanical activation in hydrometallurgy [J]. International Journal of Mineral Processing, 2003, 72(1/2/3/4): 341−354.

[14] BALAZ P, ALACOVA A, ACHIMOVICOVA M, FICERIOVA J, GODOCIKOVA E. Mechanochemistry in hydrometallurgy of sulphide minerals [J]. Hydrometallurgy, 2005, 77(1/2): 9−17.

[15] YANG Hong-ying, ZHAO Su-xing, WANG Gai-rong, ZHANG Qin, JIN Zhe-nan, TONG Lin-lin, CHEN Guo-bao, QIU Xue-min. Mechanical activation modes of chalcopyrite concentrate and relationship between microstructure and leaching efficiency [J]. Hydrometallurgy, 2022, 207: 105778.

[16] ZHANG Lei, GUO Xue-yi, TIAN Qing-hua, LI Dong, ZHONG Shui-ping, QIN Hong. Improved thiourea leaching of gold with additives from calcine by mechanical activation and its mechanism [J]. Minerals Engineering, 2022, 178: 107403.

[17] XIANG Jun-yi, HUANG Qing-yun, LV Xue-wei, BAI Chen-guang. Extraction of vanadium from converter slag by two-step sulfuric acid leaching process [J]. Journal of Cleaner Production, 2018, 170: 1089−1101.

[18] BAFGHI M S, EMAMI A H, ZAKERI A. Effect of specific surface area of a mechanically activated chalcopyrite on its rate of leaching in sulfuric acid−ferric sulfate media [J]. Metallurgical and Materials Transactions B, 2013, 44(5): 1166−1172.

[19] LI Yu-biao, WANG Bing, XIAO Qing, LARTEY C, ZHANG Qi-wu. The mechanisms of improved chalcopyrite leaching due to mechanical activation [J]. Hydrometallurgy, 2017, 173: 149−155.

[20] GRANATA G, TAKAHASHI K, KATO T, TOKORO C. Mechanochemical activation of chalcopyrite: Relationship between activation mechanism and leaching enhancement [J]. Minerals Engineering, 2019, 131: 280−285.

[21] BAI Yun-long, WANG Wei, ZHAO Shan-rong, LU Dian-kun, XIE Feng, DREISINGER D. Effect of mechanical activation on leaching behavior and mechanism of chalcopyrite [J]. Mineral Processing and Extractive Metallurgy Review, 2022, 43(4): 440−452.

[22] FAN Yang-yang, LIU Yan, NIU Li-ping, JING Ting-le, ZHANG Ting-an. Effect of mechanical activation on leaching of zinc and indium from indium-bearing zinc ferrite with sulphur dioxide as leachant and reductant [J]. Canadian Metallurgical Quarterly, 2021, 60(3): 150−159.

[23] ZHANG Cheng-long, ZHAO You-cai. Mechanochemical leaching of sphalerite in an alkaline solution containing lead carbonate [J]. Hydrometallurgy, 2009, 100(1/2): 56−59.

[24] ZHAO Zhong-wei, LONG Shuang, CHEN Ai-liang, HUO Guang-sheng, LI Hong-gui, JIA Xi-jun, CHEN Xing-yu. Mechanochemical leaching of refractory zinc silicate (hemimorphite) in alkaline solution [J]. Hydrometallurgy, 2009, 99(3/4): 255−258.

[25] CHEN Ya-jing, YANG Hong-ying, LIU Yan-hua, CHEN Guo-bao. Structural evolution of arsenopyrite and dearsenification by mechanical activation [J]. Journal of Environmental Chemical Engineering, 2021, 9(1): 104682.

[26] POURGHAHRAMANI P, AKHGAR B N. Characterization of structural changes of mechanically activated natural pyrite using XRD line profile analysis [J]. International Journal of Mineral Processing, 2015, 134: 23−28.

[27] HASHEMZADEHFINI M, FICERIOVA J, ABKHOSHK E, SHAHRAKI B K. Effect of mechanical activation on thiosulfate leaching of gold from complex sulfide concentrate [J]. Transactions of Nonferrous Metals Society of China, 2011, 21(12): 2744−2751.

[28] ZHAO Su-xing, WANG Gai-rong, YANG Hong-ying, CHEN Guo-bao, QIU Xue-min. Agglomeration−aggregation and leaching properties of mechanically activated chalcopyrite [J]. Transactions of Nonferrous Metals Society of China, 2021, 31(5): 1465−1474.

[29] KONNO H, NANRI Y, KITAMURA M. Crystallization of aragonite in the causticizing reaction [J]. Powder Technology, 2002, 123(1): 33−39.

[30] RUDNIK E. Recovery of zinc from zinc ash by leaching in sulphuric acid and electrowinning [J]. Hydrometallurgy, 2019, 188: 256−263.

[31] CHEN Ai-liang, LI Meng-chun, QIAN Zhen, MA Yu-tian, CHE Jian-yong, MA Ya-lin. Hemimorphite ores: A review of

processing technologies for zinc extraction [J]. JOM, 2016, 68(10): 2688−2697.
[32] XIA D K, PICKLES C A. Kinetics of zinc ferrite leaching in caustic media in the deceleratory period [J]. Minerals Engineering, 1999, 12(6): 693−700.
[33] ZHAO You-cai, STANFORTH R. Extraction of zinc from zinc ferrites by fusion with caustic soda [J]. Minerals Engineering, 2000, 13(13): 1417−1421.
[34] ZHANG Cheng-long, ZHAO You-cai, GUO Cui-xiang, HUANG Xi, LI Hong-jiang. Leaching of zinc sulfide in alkaline solution via chemical conversion with lead carbonate [J]. Hydrometallurgy, 2008, 90(1): 19−25.
[35] ZHANG Cheng-long, WANG Jin-wei, BAI Jian-feng, ZHAO You-cai. Recovering of zinc from solid waste bearing sphalerite or zinc ferrite by mechano-chemical extraction in alkaline solution [J]. Procedia Environmental Sciences, 2012, 16: 786−790.
[36] ZHAO You-cai, STANFORTH R. Production of Zn powder by alkaline treatment of smithsonite Zn−Pb ores [J]. Hydrometallurgy, 2000, 56(2): 237−249.
[37] ZHAO You-cai, STANFORTH R. Selective separation of lead from alkaline zinc solution by sulfide precipitation [J]. Separation Science and Technology, 2001, 36(11): 2561−2570.
[38] LENZ D M, MARTINS F B. Lead and zinc selective precipitation from leach electric arc furnace dust solutions [J]. Matéria (Rio de Janeiro), 2007, 12(3): 503−509.
[39] LI Jia-jie, HITCH M. Mechanical activation of magnesium silicates for mineral carbonation: A review [J]. Minerals Engineering, 2018, 128: 69−83.
[40] MUCSI G. A review on mechanical activation and mechanical alloying in stirred media mill [J]. Chemical Engineering Research and Design, 2019, 148: 460−474.

机械力化学浸出法从氧化锌矿中高效浸出锌

余裕森[1,2]，崔立雪[1,2]，张利波[1,2]，王云帆[1,2]

1. 昆明理工大学 冶金与能源工程学院，昆明 650093；
2. 昆明理工大学 省部共建复杂有色金属资源清洁利用国家重点实验室，昆明 650093

摘　要：以篮式研磨机为机械力化学活化设备对我国兰坪地区低品位氧化铅锌矿进行研究，提出将研磨与 NaOH 溶液浸出过程相结合浸出锌的机械力化学浸出(MCL)工艺。研究浸出温度、NaOH 浓度、浸出时间、液固比和搅拌速度对锌浸出率的影响。实验结果表明，在最佳浸出条件下，采用 MCL 工艺锌的浸出率达到 92.3%，比常规搅拌浸出(CSL)工艺的高 7.2%，且两种工艺的能耗相差不大，证明了 MCL 工艺的优越性。通过对原矿进行锌物相分析以及对最佳条件下不同工艺浸出渣进行 XRD、SEM–EDS、EPMA 和粒度等分析，研究机械力化学活化的强化机理。

关键词：机械力化学浸出；机械活化；碱浸出；氧化锌矿；篮式研磨机

(Edited by Wei-ping CHEN)